iScience

CellPress
OPEN ACCESS

Article

PEGylated talazoparib enhances therapeutic window of its combination with temozolomide in Ewing sarcoma

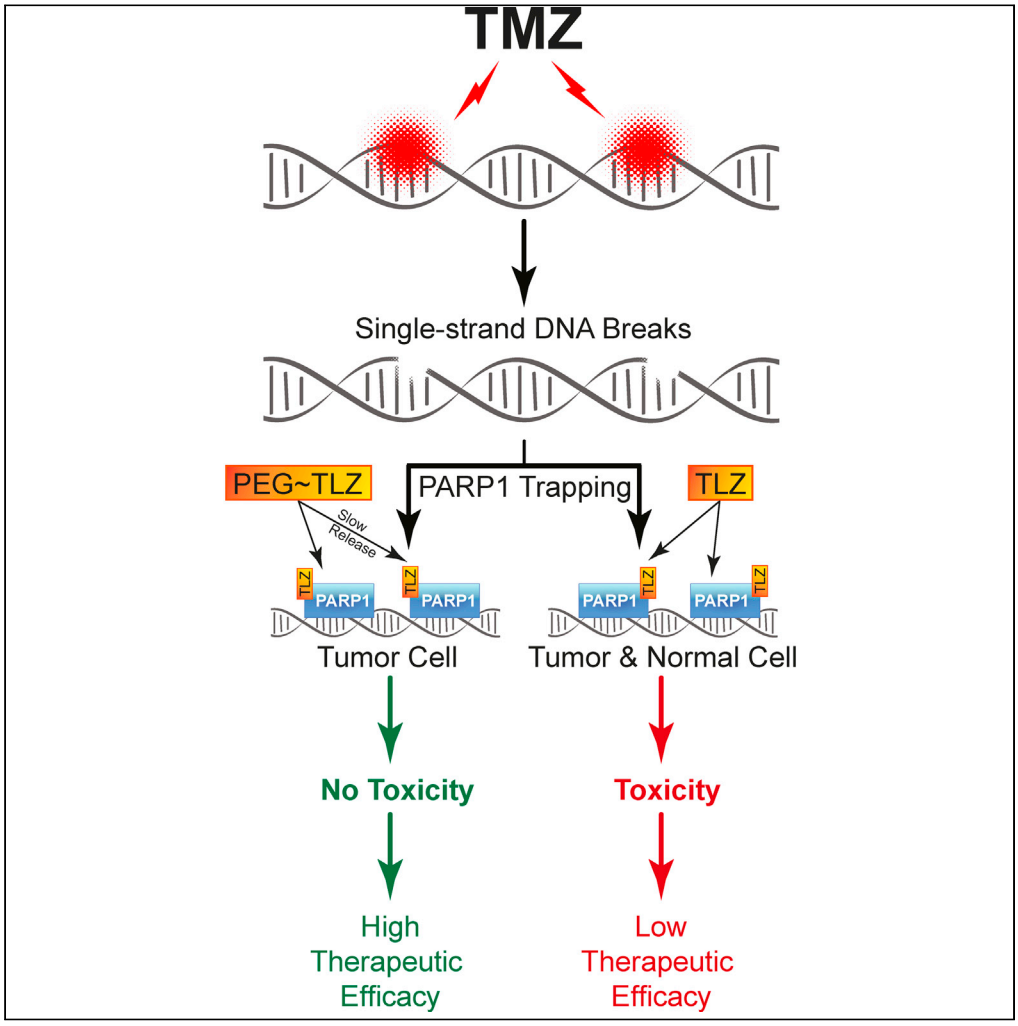

Vanessa Del Pozo, Andrew J. Robles, Shaun D. Fontaine, Qianqian Liu, Joel E. Michalek, Peter J. Houghton, Raushan T. Kurmasheva

Kurmasheva@uthscsa.edu

Highlights

Nanoparticle-formulated drugs minimize drug-induced toxicity

PEG~TLZ enhances *in vivo* activity of TMZ in pediatric tumor xenografts

A 3-day interval between each drug's administration widens the therapeutic window

A single IV dose of PEG~TLZ is advantageous for treating infants/young children

Del Pozo et al., iScience *25*, 103725
February 18, 2022
https://doi.org/10.1016/j.isci.2021.103725

iScience

CellPress
OPEN ACCESS

Article

PEGylated talazoparib enhances therapeutic window of its combination with temozolomide in Ewing sarcoma

Vanessa Del Pozo,[1,6] Andrew J. Robles,[1,6] Shaun D. Fontaine,[2] Qianqian Liu,[3] Joel E. Michalek,[3] Peter J. Houghton,[1,4] and Raushan T. Kurmasheva[1,4,5,7,*]

SUMMARY

Current therapy is ineffective for relapsed and metastatic Ewing sarcoma (EwS) owing to development of drug resistance. Macromolecular prodrugs potentially lead to lower drug exposure in normal tissues and reduced toxicity. We evaluated the efficacy of PEGylated talazoparib (PEG∼TLZ), a PARP1 inhibitor, alone or in combination with the DNA-alkylating agent temozolomide (TMZ) in EwS and other pediatric tumors using conventional testing or single-mouse trial (SMT). A single dose of PEG∼TLZ (10 μmol/kg on day 0) combined with 5 daily doses of TMZ (40 mg/kg starting on day 3/4) produced minimal toxicity, and the combination achieved maintained complete response in EwS and glioblastoma models. The SMT trial with the 3-day interval between PEG∼TLZ and TMZ resulted in objective responses in EwS and other xenografts. Thus, PEG∼TLZ + TMZ demonstrated a broad range of activity in pediatric solid tumor models. Furthermore, the therapeutic window of PEG∼TLZ + TMZ was enhanced compared with the free-TLZ combination.

INTRODUCTION

Although intensive chemotherapy can result in sustained event-free survival (EFS) and overall survival for children and young adults with Ewing sarcoma, this regimen is relatively ineffective for relapsed and metastatic Ewing sarcoma, for which overall long-term survival ranges from 9% to 33% (Kolb et al., 2003; Potratz et al., 2012). Current Ewing sarcoma standard treatment protocols include five chemotherapeutics (cyclophosphamide, vincristine, etoposode, doxorubicin, and ifosfamide), plus radiation (Donaldson et al., 1998; Dunst et al., 1995; Ferrari et al., 1998; Grier et al., 2003; Krasin et al., 2004). Four of these drugs induce DNA damage, as does radiation therapy. At relapse, two additional DNA-damaging agents (irinotecan and temozolomide [TMZ]) are routinely used to re-induce remission, indicating that Ewing sarcoma cells are intrinsically sensitive to DNA damage. However, the standard of care for Ewing sarcoma has not significantly changed in the last ∼30 years, with many chemotherapeutics triggering toxicities to normal tissues due to the DNA damaging effects. Recent preclinical and clinical trials of the experimental combination of talazoparib (TLZ), the most potent of the approved PARP1 inhibitors, and TMZ in Ewing sarcoma demonstrated notable antitumor activity, but the combination was toxic both in patients and in mice (Schafer et al., 2020; Smith et al., 2015). As an alternative therapeutic approach to reducing toxicity and improving efficacy of the drug combination, we evaluated a novel PEGylated conjugate of TLZ (PEG∼TLZ) that allows sustained, controlled release of the inhibitor within the tumor microenvironment (Fontaine et al., 2021). Nanocarrier-linked drugs increase uptake into tumor tissue and reduce permeability to normal vasculature, leading to lower dose exposure in normal tissues and reduced toxicity (Van De Ven et al., 2017, Caster et al., 2015; Tsouris et al., 2014; Maeda et al., 2000; Baldwin et al., 2019; Chauhan and Jain, 2013; Chauhan et al., 2012; Matsumura and Maeda, 1986; Yang et al., 2021). The enhanced permeability and retention effect is specific to passive systemic distribution of nanomedicine and allows selective penetration of drugs due to the increased vascular pore size in the tumor site (Maeda et al., 2000). In this study, the *in vivo* activity of PEG∼TLZ was assessed in Ewing sarcoma xenograft models and an MGMT-deficient model of glioblastoma using conventional testing (10 mice/group) and in an extended group of pediatric solid tumors using a single-mouse testing (SMT) approach (1 mouse/group).

[1]Greehey Children's Cancer Research Institute, UT Health San Antonio, San Antonio, TX 78229, USA

[2]ProLynx Inc., South San Francisco, CA 94158, USA

[3]Department of Population Health Sciences, UT Health San Antonio, San Antonio, TX 78229, USA

[4]Department of Molecular Medicine, UT Health San Antonio, San Antonio, TX 78229, USA

[5]Senior author

[6]These authors contributed equally

[7]Lead contact

*Correspondence: Kurmasheva@uthscsa.edu

https://doi.org/10.1016/j.isci.2021.103725

A-673

	TMZ	TMZ+PEG-TLZ
IC50 absolute (uM)	331.8	6.235

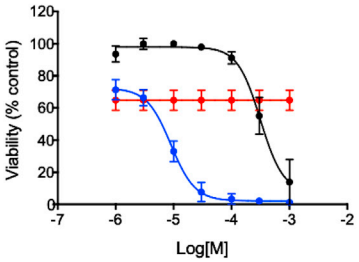

TC-71

	TMZ	TMZ+PEG-TLZ
IC50 absolute (uM)	165.6	9.959

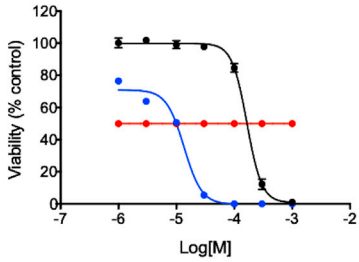

EW8

	TMZ	TMZ+PEG-TLZ
IC50 absolute (uM)	243.8	5.520

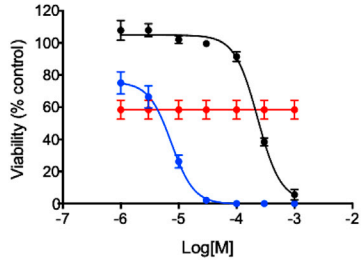

ES-4

	TMZ	TMZ+PEG-TLZ
IC50 absolute (uM)	85.90	10.30

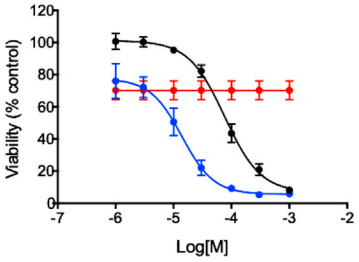

ES-2

	TMZ	TMZ+PEG-TLZ
IC50 absolute (uM)	15.68	3.909

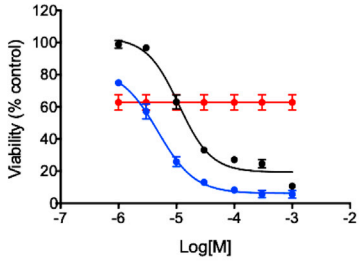

CHLA-258

	TMZ	TMZ+PEG-TLZ
IC50 absolute (uM)	141.2	8.940

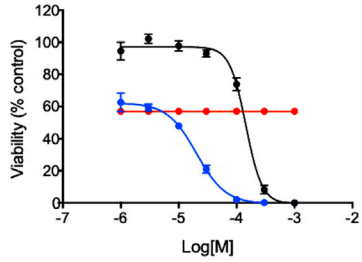

ES-7

	TMZ	TMZ+PEG-TLZ
IC50 absolute (uM)	175.2	3.520

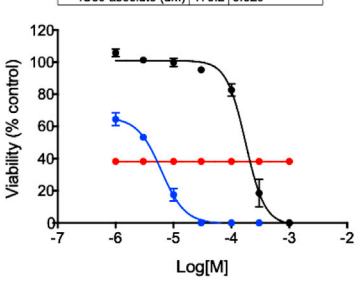

ES-6

	TMZ	TMZ+PEG-TLZ
IC50 absolute (uM)	301.6	8.064

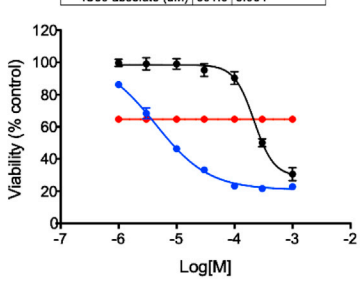

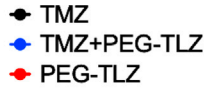

Bliss Combination Indices

Cell Line	10 μM TMZ + PEG~TLZ (IC_{50})	30 μM TMZ + PEG~TLZ (IC_{50})	100 μM TMZ + PEG~TLZ (IC_{50})
ES-4	0.67	0.54	0.77
ES-7	0.75	0.64	0.68
TC-71	1.02	0.54	0.58
EW-8	0.55	0.43	0.47
ES-6	0.67	0.57	0.54
A-673	0.53	0.40	0.42
CHLA-258	0.85	0.59	0.59
ES-2	0.82	0.91	0.90

Figure 1. Ewing sarcoma cell lines sensitivity to TMZ and PEG∼TLZ + TMZ

Alamar Blue concentration-response curves.Cells were treated for 72 h with indicated concentrations of TMZ alone or in combination with a single concentration of PEG∼TLZ. The red line in each graph indicates the effect of PEG∼TLZ alone at the concentration used in combination with TMZ. Results represent mean ± SEM for n = 3 independent experiments, with each concentration tested in triplicate. *Bottom,* Table with the Bliss combination indices for PEG∼TLZ + TMZ. See also Figure S1 and Table S1.

RESULTS

In vitro potentiation of TMZ by PEG∼TLZ

Our previous results, generated in the Pediatric Preclinical Testing Program (PPTP), showed that Ewing sarcoma xenografts segregated into two groups with five models showing dramatic antitumor activity of TLZ and TMZ and four models where the combination was inactive (Smith et al., 2015). To understand the mechanisms accounting for the difference in activity to the combination of PARP1 inhibition and DNA damage observed in Ewing sarcoma xenografts, we first examined synergy between PEG∼TLZ and TMZ *in vitro*. It has been argued, based on preclinical (Shen et al., 2013) and clinical (Drew et al., 2016) evidence, that optimal efficacy of PARP1 inhibitors requires continuous inhibition of PARP1. To accomplish protracted drug exposure, we used a four-arm PEG_{40kDa} nanocarrier (15 nm diameter) conjugated to TLZ via a releasable linker developed by ProLynx. In this PEGylated prodrug, the release of TLZ is determined by the modulator group. TLZ was released with an *in vitro* $t_{1/2}$ ∼160 h at pH 7.4, 37°C (Fontaine et al., 2021).

We first investigated the degree of potentiation of TMZ cytotoxicity by PEG∼TLZ in the Ewing sarcoma cell lines ES-2, ES-4, ES-6, ES-7, EW-8, A-673, CHLA-258, and TC-71 (Figure 1, Figure S1). Cells were exposed to increasing concentrations of TMZ, with or without co-treatment with PEG∼TLZ (approximate IC_{50}), for 72 h, and cell viability was assessed by Alamar Blue staining. Treatment with PEG∼TLZ + TMZ resulted in increased cytotoxicity compared with TMZ alone in all the models evaluated. The IC_{50} values for TMZ alone ranged from 15.7 μM in ES-2 cells to 331.8 μM in A-673 cells. In contrast, the IC_{50} values for TMZ combined with the IC_{50} of PEG∼TLZ ranged from 3.5 μM in ES-7 cells to 10.3 μM in ES-4 cells (Table 1, Figure 1). Overall, these results suggest that the combination of PEG∼TLZ + TMZ more potently inhibits cell viability compared with TMZ alone. Using these same data, we next asked whether the combination of PEG∼TLZ + TMZ produces greater than additive cytotoxic effects, which would suggest a synergistic interaction. We chose to evaluate concentrations of 10, 30, and 100 μM TMZ when measuring synergy with PEG∼TLZ because these concentrations span the dynamic range of relevant concentrations *in vitro*. In addition, these concentrations are clinically relevant as micromolar concentrations of TMZ can be detected in patient plasma following TMZ administration (Britten et al., 1999; Portnow et al., 2009). Interesting, the effects of several combinations of PEG∼TLZ + TMZ were significantly greater than would be expected if the effects of each drug were simply additive in ES-6, ES-7, EW-8, ES-2, and A-673 cells (Figure S1). In particular, greater than additive effects were observed when combining PEG∼TLZ (IC_{50}) with 100 μM TMZ in ES-6, ES-7, EW-8, ES-2, and A-673 cells. Greater than additive effects were also observed when combining PEG∼TLZ with 30 μM TMZ in ES-6, ES-7, EW-8, ES-2, and A-673 cells and when combining PEG∼TLZ with 10 μM TMZ in ES-6, ES-7, EW8, and A-673 cells. Furthermore, we calculated combination indices (CIs) for these combinations based on the Bliss model of independence (Bliss, 1939). CIs for PEG∼TLZ (IC_{50}) with 10, 30, or 100 μM TMZ ranged from 0.40 to 1.02 (Figure 1). These data suggest various degrees of synergy between the combination, with lower CI values (greater synergy) typically observed at higher TMZ concentrations. Overall, these results suggest a synergistic interaction between PEG∼TLZ and TMZ in some Ewing sarcoma cell lines, particularly at higher concentrations of TMZ.

Apoptosis induction

We next evaluated the induction of apoptosis by PEG∼TLZ, TMZ, and PEG∼TLZ + TMZ by evaluating PARP1 cleavage in ES-2, ES-4, ES-6, ES-7, EW-8, A-673, CHLA-258, and TC-71 cells after 24 and 48 h of treatment (Figure 2). We sought to identify the time points (24 and 48 h) at which PARP1 cleavage could be first detected. After 24 h of treatment, cleaved PARP1 was detectable only after combination treatment, but not PEG∼TLZ or TMZ treatment, in ES-4, ES-7, A-673, and TC-71. In CHLA-258 cells, PARP1 cleavage was detectable after treatment with either single agent or the combination, whereas in EW-8 cells PARP1 cleavage was only detected in TMZ- and combination-treated cells. In ES-2 cells, PARP1 cleavage was only detected after 24 h of TMZ-treatment. After 48 h of treatment, cleaved PARP1 was detectable with TMZ or the combination treatment, but not PEG∼TLZ, in ES-2, ES-4, and EW-8 cells. In contrast, PARP1 cleavage was detectable 48 h after treatment with either single agent or the combination in ES-7, A-673, and TC-71 cells. In ES-6 cells, cleaved PARP1 was only detectable in combination-treated cells. Although the magnitude of

Table 1. Potentiation of TMZ cytotoxicity by PEG∼TLZ

Cell line	TMZ IC_{50} (μM)	TMZ + PEG∼TLZ IC_{50} (μM)	Potentiation factor (fold)
ES-4	85.9	10.3	8.3
ES-7	175.2	3.5	50.1
TC-71	165.6	10.0	16.6
EW-8	243.8	5.5	44.3
ES-6	301.6	8.1	37.2
A-673	331.8	6.2	53.5
CHLA-258	141.2	8.9	15.9
ES-2	15.7	3.9	4.0

See also Table S1.

induction of PARP1 cleavage is not equal between the cell lines, it is possible that longer time is needed for induction of apoptosis in some of the cell lines owing to their comparatively slower growth. This is particularly true with ES-4 and ES-6 cells, which, in our experience, have doubling times greater than 24 h. Collectively, these results suggest that the combination of PEG∼TLZ + TMZ results in a more rapid and greater induction of apoptosis than either single agent in a majority of the cell lines evaluated.

Combination testing of PEG∼TLZ with TMZ in non-tumored mice

Previously we found that combining free-TLZ with TMZ resulted in significant body weight loss and mortality unless the dose of TMZ was reduced to approximately 15% of its MTD (Smith et al., 2015). The reasoning behind using PEG∼TLZ is that dosing of TMZ could be delayed as PEG∼TLZ would be retained in tumor tissue while being cleared systemically. In non-tumored mice, PEG∼TLZ at 5 and 10 μmol/kg in combination with TMZ (40 mg/kg daily for 5 days) was tolerated when TMZ was administered on days 2–6 and PEG∼TLZ administered on day 1 (Figure S2). In contrast, PEG∼TLZ at 20 μmol/kg combined with TMZ at the same dose and schedule of administration caused >20% body weight loss, hence was considered too toxic.

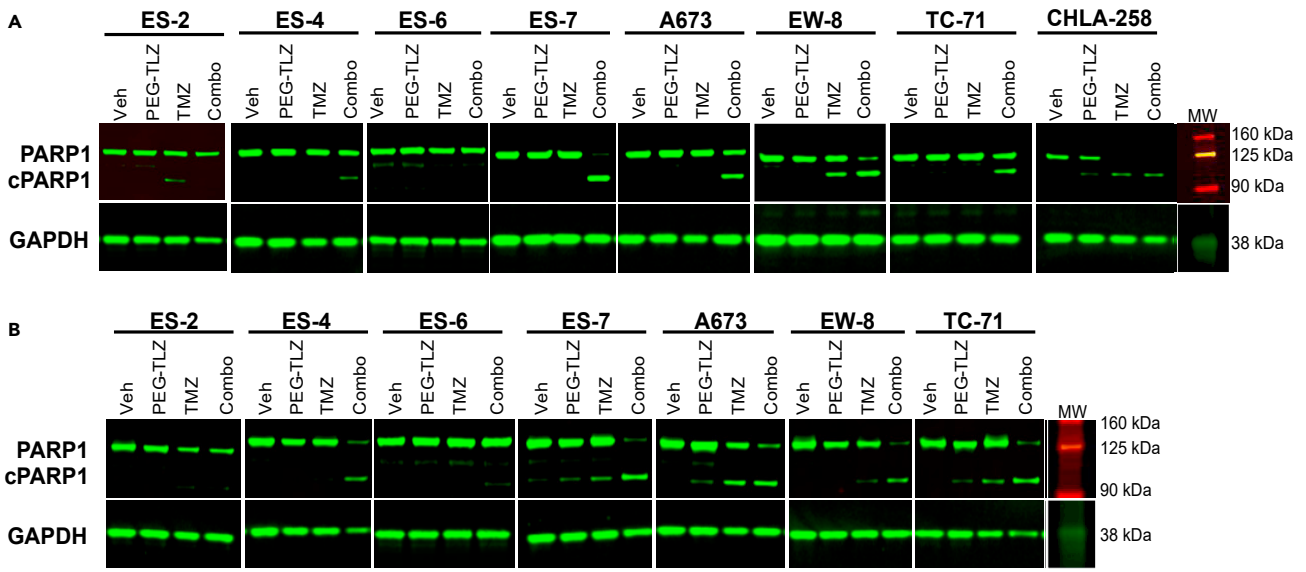

Figure 2. Induction of apoptosis in Ewing sarcoma cells by PEG∼TLZ, TMZ, and PEG∼TLZ + TMZ

(A and B) Ewing sarcoma cell lines were treated for 24 (A) or 48 h (B) with vehicle, PEG∼TLZ (IC_{50}), TMZ (IC_{50}), and PEG∼TLZ + TMZ (IC_{50} of each).PARP1 cleavage (cPARP1; 89 kDa) was evaluated by immunoblotting with PARP1 antibody (89/116 kDa). GAPDH (37 kDa) was used as a loading control. See also Table S1.

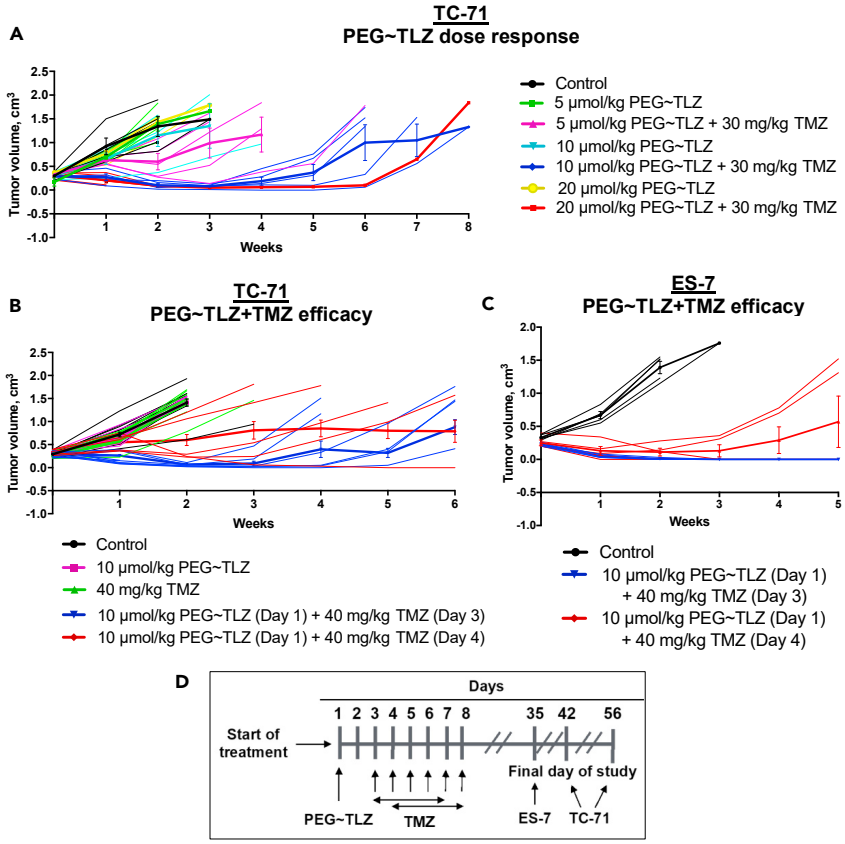

Figure 3. PEG∼TLZ + TMZ tumor activity in Ewing sarcoma-bearing mice

(A) PEG∼TLZ dose-response study: TC-71 tumor-bearing mice received various doses of PEG∼TLZ ± TMZ (30 mg/kg daily x 5) starting 3 days after single dose of PEG∼TLZ. Tumor volumes were measured for 56 days. The thinner lines represent individual mice and the bolder lines (with error bars) represent median tumor growth in each group. Error bars represent mean ± SEM. See also Figures S2 and S3.

(B) Efficacy study of PEG∼TLZ + TMZ in TC-71 model: tumor-bearing mice received PEG∼TLZ (10 µmol/kg, single dose), TMZ (40 mg/kg daily x 5), and PEG∼TLZ + TMZ (in 2 schedules, p = 0.002). Tumor volumes were measured for 42 days. The thinner lines represent individual mice and the bolder lines (with error bars) represent median tumor growth in each group. Error bars represent mean ± SEM. P-values were calculated by two-sided log rank test. See also Figures S2 and S3.

(C) Efficacy study of PEG∼TLZ + TMZ in ES-7 model: tumor-bearing mice received PEG∼TLZ, TMZ, and PEG∼TLZ + TMZ (in two schedules, p = 0.002). Tumor volumes were measured for 35 days. The thinner lines represent individual mice and the bolder lines (with error bars) represent median tumor growth in each group. Error bars represent mean ± SEM. P-values were calculated by two-sided log rank test. See also Figures S2 and S4.

(D) Drug treatment schedules scheme for the *in vivo* experiments presented in this figure. See also Figure S2.

Efficacy of PEG∼TLZ combined with TMZ in tumored mice

Initial studies in tumor-bearing mice showed that scheduling TMZ 1 day after PEG∼TLZ was too toxic (>10% body weight loss). Further studies explored delaying the start of TMZ treatment by 3 or 4 days after PEG∼TLZ administration (Figures 3 and 4; Figures S3 and S4). As shown in Figure 3A, PEG∼TLZ at doses up to 20 µmol/kg did not significantly inhibit growth of TC-71 Ewing sarcoma xenografts. TMZ, administered 3 days after PEG∼TLZ at a daily dose of 30 mg/kg, was highly active when combined with 10 and 20 µmol/kg of PEG∼TLZ. We wanted to explore whether a higher dose level of TMZ combined with lower PEG∼TLZ was equally effective, and to determine the optimal scheduling of TMZ after administration of the PARP1 inhibitor. Neither PEG∼TLZ (10 µmol/kg) nor TMZ (40 mg/kg daily x 5) had any antitumor activity against TC-71 xenografts. By contrast, the combination with TMZ administration initiated 3 days after PEG∼TLZ was effective at causing tumor regressions, whereas delaying administration of TMZ until 4 days after the PARP1 inhibitor markedly reduced antitumor activity (Figure 3B). A similar study in ES-7 Ewing sarcoma xenografts gave very similar results. Scheduling TMZ 3 days post PEG∼TLZ resulted in maintained complete response (CR) over the observation period (13 weeks), whereas when administration of

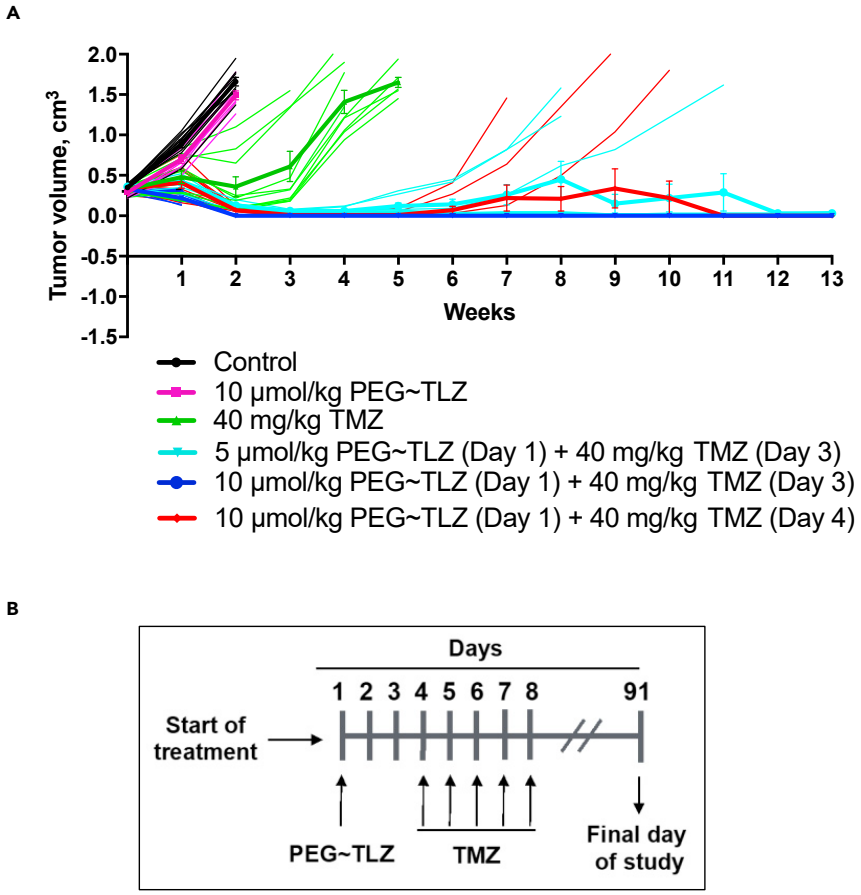

Figure 4. PEG~TLZ + TMZ efficacy in glioblastoma xenograft model

(A) GBM2 tumor-bearing mice received PEG~TLZ (10 µmol/kg, single dose), TMZ (40 mg/kg daily x 5), and PEG~TLZ + TMZ (in two schedules and two PEG~TLZ doses, $p \geq 0.002$). Tumor volumes were measured for 91 days. The thinner lines represent individual mice, and the bolder lines (with error bars) represent median tumor growth in each group. Error bars represent mean ± SEM. p-values were calculated by two-sided log rank test. See also Figures S2 and S4.

(B) Drug treatment schedule scheme for the *in vivo* testing of PEG~TLZ and TMZ in the GBM2 xenograft model. See also Figure S2.

TMZ was started 4 days after the PARP1 inhibitor the tumor response was partial response (PR) with EFS of 5 weeks (Figure 3C). Thus, the spacing of 3 days between PEG~TLZ and TMZ administration used in the xenograft models was optimal.

To explore the efficacy of PEG~TLZ in combination with TMZ in a model other than Ewing sarcoma, we used the glioblastoma GBM2 xenograft model, which is deficient in MGMT, and thus sensitive to TMZ (Middlemas et al., 2000). In this tumor model, TMZ induced significant growth delay (EFS = 28 days; $p = 0.002$), whereas PEG~TLZ as a single agent had no antitumor activity (10 µmol/kg), Figure 4. TMZ administered on days 3–7 after PEG~TLZ induced maintained CR at the end of the study (10 weeks), whereas reducing the dose of PEG~TLZ to 5 µmol/kg resulted in a significant loss of antitumor activity ($p = 0.005$), a result similar to the combination using 4-day spacing between TMZ and PEG~TLZ, which was less active ($p = 0.002$).

Evaluation of PEG~TLZ combined with TMZ using single-mouse testing

We have previously used the SMT study design to encompass tumor models with greater diversity and molecular heterogeneity (Ghilu et al., 2020; Kendsersky et al., 2021), based on a retrospective analysis of >2,100 studies undertaken by the PPTP that showed that a single mouse accurately predicts group response (n = 10) in conventional testing in 78% of studies. Prospective testing in solid tumor and leukemia patient-derived xenografts PDXs has confirmed the utility of SMT (Houghton et al., 2020). We evaluated the

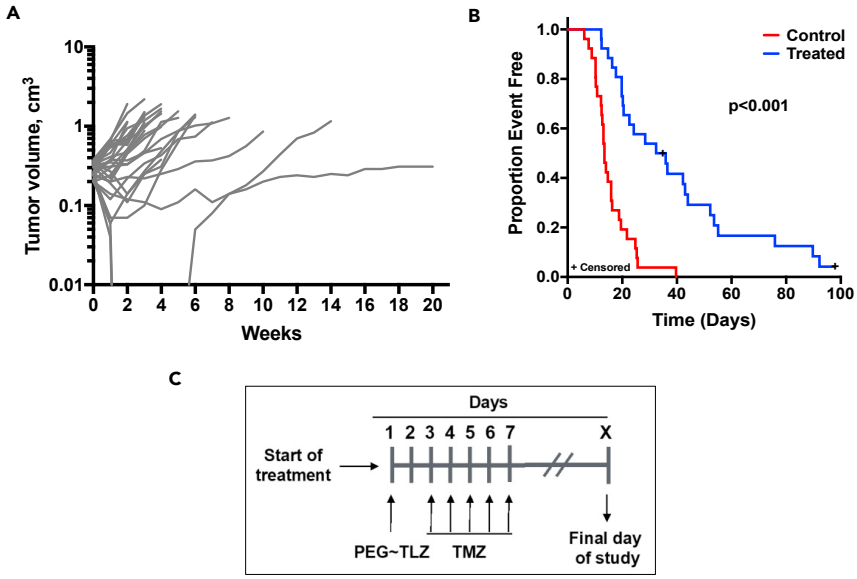

Figure 5. Single-mouse testing of PEG∼TLZ + TMZ in pediatric xenograft tumor models

(A) Antitumor activity to the combination of PEG∼TLZ + TMZ in 28 xenograft models. Tumor volumes were measured for up to 140 days. See also Figure S2 and Table S2.

(B) Kaplan-Meier EFS curves for control versus treated groups. Tumor volumes were measured weekly for up to 100 days ($p < 0.001$). p-value was calculated by the two-sided log rank test. See also Figure S2 and Table S2.

(C) Drug treatment schedule scheme for the *in vivo* single-mouse testing study with PEG∼TLZ (10 μmol/kg, single dose, on day 0) and TMZ (40 mg/kg x 5 days starting on day 3) in Ewing sarcoma, osteosarcoma, rhabdomyosarcoma, malignant rhabdoid tumor, and synovial sarcoma xenograft models. X, final day varies depending on the model. See also Figure S2 and Table S2.

combination of PEG∼TLZ (10 μmol/kg) and TMZ (40 mg/kg daily x 5) using 3-day spacing between drug administrations in an additional 28 tumor models (including 12 Ewing sarcoma, 8 rhabdomyosarcoma, 3 malignant rhabdoid tumors, 1 Wilms tumor, 1 osteosarcoma, and 3 synovial sarcoma) (Figure 5, Table S2). There was one drug-related death; however, the Kaplan-Meier survival curve demonstrated that the PEG∼TLZ + TMZ treatment caused extended survival compared with the EFS for untreated tumors for the same models. The median EFS for control (n = 26) versus treated groups (n = 26) was estimated to be 13.5 and 34.2 days, respectively (with confidence interval of (12.2, 15.9) and (20.2, 44) for each group). We observed 7 objective responses (5 PR, 1 CR, 1 MCR; 22.6%); 3 tumor lines were considered stable disease (SD [<50% regression, <25% volume increase]); and 21 models progressed on treatment (PD). Time to event (defined as the day a tumor achieved 400% of its volume on the day of treatment) varied from 12 days to >161 days (Table 2).

DISCUSSION

Ewing sarcoma is an aggressive pediatric cancer that arises in bone and soft tissues. Despite many attempts to develop an effective treatment over the last three decades, current standard therapy is not effective against the relapsed and metastatic disease. In a prior study by the PPTP, the combination of free TLZ with TMZ showed CR and maintained CR in half of the tested Ewing sarcoma xenograft models (Smith et al., 2015). However, the synergistic response was associated with significant toxicity, which necessitated reduction of the TMZ dose to ∼15% of its MTD. Similarly, the Children's Oncology Group phase I/II clinical trial yielded high toxicity but SD and PR in a limited number of patients (Schafer et al., 2020). An important future direction for an efficacious Ewing sarcoma therapy could be employing a controlled passive delivery of nanomedicines to tumor sites, which allows significant reductions in systemic toxicity. We were therefore interested in whether PEG∼TLZ would enhance the therapeutic window of its combination with TMZ in Ewing sarcoma and other pediatric solid tumor xenograft models. Although the pharmacodynamic testing was not performed, the TLZ dose utilized in our earlier study (0.165 mg/kg BID x 5 days of free TLZ [cumulative 1.65 mg/kg] versus 5 and 10 μmol/kg single dose of PEG∼TLZ in this study [equivalent to 1.9 and

Table 2. Summary of SMT results

Xenograft	Histology	EFS,[a] control (days)	EFS, treated (days)	Response[b]
CHLA-258	Ewing sarcoma	16.3	>98	MCR
SK-NEP1	Ewing sarcoma	10.2	24.2	PD
[c]NCH-EWS1	Ewing sarcoma	10.3	28.4	PD
ES-1	Ewing sarcoma	12.4	42.2	PR
ES-2	Ewing sarcoma	14.7	52.2	PR
ES-3	Ewing sarcoma	13.5	19.8	PD
ES-4	Ewing sarcoma	12.2	12.3	PD
ES-6	Ewing sarcoma	21.7	43.0	SD
[c]EW-5	Ewing sarcoma	13.1	14.8	PD
EW-8	Ewing sarcoma	6.1	44.0	SD
[c]EW-10	Ewing sarcoma	NA	>161	PR
[c]EW-13	Ewing sarcoma	25.3	53.6	PD
[c]WT-16	Wilms tumor	13.1	89.8	PD
[c]RBD2	MRT	7.7	12.4	PD
[c]WT-14	MRT	25.6	92.2	CR
[c]Rh-18	MRT	19.5	55.1	PR
[c]Rh-28	ARMS	18.8	20.2	PD
[c]Rh-30R	ARMS	13.5	35.9	PD
[c]Rh-41	ARMS	10.8	22.6	PD
[c]Rh-65	ARMS	12.7	19.8	PD
[c]Rh-73	ERMS	24.8	36.5	PR
[c]Rh-80	ERMS	8.8	20.5	PD
[c]Rh-82	ARMS	10.2	32.4	PD
[c]Rh-88	ERMS	15.9	17.7	PD
[c]OS-46	Osteosarcoma	39.7	75.9	SD
ASKA-SS	Synovial sarcoma	15.9	16.3	PD
Yamato-SS	Synovial sarcoma	NA	21.1	PD
HS-SY-II	Synovial sarcoma	14	>35	PD

See also Table S2.

Limited demographics data for the models in this table are published (https://pedcbioportal.kidsfirstdrc.org and in (Rokita et al., 2019)).

MRT, malignant rhabdoid tumor; ERMS, embryonal rhabdomyosarcoma; ARMS, alveolar rhabdomyosarcoma; N/A, data not available.

[a]EFS, event-free survival. An "event" is defined as a quadrupling of tumor volume from day 0. The exact time-to-event is estimated by interpolating between the measurements directly preceding and following the event, assuming log-linear growth.

[b]Progressive disease (PD) is defined as >25% increase in initial volume within 21 days of starting treatment. Stable disease (SD) is defined as <50% regression from initial volume during the study period and ≤25% increase in initial volume within 21 days of starting treatment. Partial response (PR) is defined as a tumor volume regression ≥50% for at least one time point but with measurable tumor (0.04 cm^3). Complete response (CR) is defined as the disappearance of measurable tumor mass (<0.04 cm^3) for at least one time point. A complete response is considered maintained (MCR) if the tumor volume is <0.04 cm^3 at the end of the study period.

[c]Designates patient-derived xenograft (PDX) models.

3.8 mg/kg]) has been shown to induce apoptosis in the PALB2-mutated Wilms tumor xenograft (KT-10) responsive to TLZ treatment (Baldwin et al., 2019).

We previously showed that PEG∼TLZ maintains a controlled and slow release of TLZ over ∼1 week in mice (Fontaine et al., 2021). Furthermore, the long elimination half-life, high tumor uptake, and very low efflux rates from tumors have been validated by PET imaging of PEG_{40kDa}-^{89}Zr conjugates (Beckford Vera et al., 2020). Key parameters for a high therapeutic index of a single drug/drug combination are low or

undetectable toxicity and a strong tumor response to therapy. Our initial toxicity testing of PEG∼TLZ in non-tumor-bearing mice demonstrated that single doses of 5 and 10 μmol/kg, equivalent to 1.9 and 3.8 mg/kg of free TLZ, can be safely administered with TMZ at 40 mg/kg (<10% weight loss). When TLZ was given as free drug in the PPTP study, a similar dose of TLZ (0.33 mg/kg x 5 days = 1.65 mg/kg) resulted in >20% weight loss when combined with 16 mg/kg of TMZ (Smith et al., 2015). Furthermore, consistent with our *in vitro* cytotoxicity results demonstrating TMZ potentiation by PEG∼TLZ in Ewing sarcoma cell lines, the studies of mice bearing Ewing sarcoma revealed that the 3-day delay in TMZ administration (after PEG∼TLZ given on day 0) was more efficacious (maintained CR) compared with the 4-day delay schedule (PR). This difference in response is possibly due to the PEG∼TLZ pharmacokinetics. Similarly, maintained CR was achieved with PEG∼TLZ + TMZ using the 3-day delayed schedule in a glioblastoma xenograft model, providing evidence for high activity of this drug combination in other pediatric solid tumors. The single-mouse testing (SMT) of PEG∼TLZ + TMZ in 28 models including Ewing sarcoma, malignant rhabdoid tumor, Wilms tumor, rhabdomyosarcoma, osteosarcoma, and synovial sarcoma xenografts demonstrated a range of antitumor activity, with 7 models (22.6%) showing objective responses in Ewing sarcoma and malignant rhabdoid tumor models that carry *SMARCB1* gene homozygous deletions. The median EFS for this series of treated tumors was 35.9 days, whereas the median for model paired untreated tumors was 13.5 days.

Although xenografts in immunodeficient mice have limitations in that there is no immune system that can contribute to tumor response, they more accurately represent human cancers than other available models. In this study we used heterotopic (subcutaneous) transplantation rather than orthotopic transplantation, hence potentially the tumor microenvironment may differ contributing to the response to therapy. Although this may apply to brain tumors where drug access to the intracranial model may be restricted, there is less compelling evidence for non-brain tumors. The microenvironment may influence drug response; however, our expression profiling shows subcutaneous tumor xenografts cluster with their appropriate human cancers, which by definition have to be ''orthotopic,'' suggesting that changes in subcutaneous tumor microenvironment may have a relatively modest effect on cancer cell expression (Neale et al., 2008).

In summary, PEG∼TLZ + TMZ demonstrated enhanced *in vivo* activity of TMZ in xenograft models when administered 3 days prior to TMZ. SMT revealed antitumor activity against malignant rhabdoid tumor models for this drug combination dose and schedule. Thus, the addition of PEG∼TLZ to standard-of-care TMZ may widen the therapeutic index of the combination for Ewing sarcoma and other pediatric solid tumors. Along with significant reduction in toxicity, single dosing of PEG∼TLZ may be advantageous for treating infants and young children when compared with free TLZ given orally for 28 days.

Limitations of the study

Although the tumor microenvironment may differ from the natural site of tumor occurrence, xenograft models in immunodeficient mice were used in the study because they more accurately represent human cancers than other available models (also addressed in discussion). Testing data for the combination of free TLZ and TMZ in pediatric solid tumor xenografts referenced in this work are from previous study (Smith et al., 2015); however, the same *in vivo* methods were used in both (Houghton et al., 2007; Murphy et al., 2016). In addition, the varied growth rate between the cell lines in this study may affect the timing of PARP1 cleavage, an early apoptosis marker (also addressed in results).

STAR★METHODS

Detailed methods are provided in the online version of this paper and include the following:

- KEY RESOURCES TABLE
- RESOURCE AVAILABILITY
  - Lead contact
  - Materials availability statement
  - Data and code availability
- EXPERIMENTAL MODEL AND SUBJECT DETAILS
  - Ewing sarcoma cell lines and solid tumor xenograft models
- METHOD DETAILS
  - *In vitro* cytotoxicity assay

SUPPLEMENTAL INFORMATION

Supplemental information can be found online at https://doi.org/10.1016/j.isci.2021.103725.

ACKNOWLEDGMENTS

We thank Yuzuru Shiio, PhD for providing synovial sarcoma cell lines; Daniel Santi, MD, PhD for providing PEG~TLZ; and Abhik Bandyophadhyay, PhD, Samson Ghilu, Edward Favors, and Kevin Brown for technical assistance. This study was supported in part by RP160716 from the Cancer Prevention and Research Institute of Texas (CPRIT), P01CA165995-03 from the National Cancer Institute (NCI), 1U01CA263981-01 from the NCI, RP170345 Cancer Biology Training Program from the CPRIT, T32CA148724 from the NCI, the Greehey Children's Cancer Research Institute (GCCRI) PDX and Cell Lines Core, and the GCCRI.

AUTHOR CONTRIBUTIONS

R.T.K. conceived the research; R.T.K. and P.J.H. designed the experiments; V.D.P. and A.J.R. performed the experiments; Q.L., A.J.R., J.E.M., P.J.H., and R.T.K. analyzed data; R.T.K. and P.J.H. wrote the manuscript; and S.D.F., A.J.R., and J.E.M. edited the manuscript.

DECLARATION OF INTERESTS

S.D.F. was a paid employee (currently a paid consultant) of Prolynx, LLC at the time of work performance and manuscript preparation and holds options to purchase shares of Prolynx, LLC. PEG~TLZ is covered under the patent application WO2021041964A1 (by Prolynx, LLC). All other authors declare that they have no conflicts of interest to disclose.

INCLUSION AND DIVERSITY

We worked to ensure diversity in experimental samples through the selection of the cell lines. One or more of the authors of this paper self-identifies as an underrepresented ethnic minority in science.

Received: August 3, 2021
Revised: November 14, 2021
Accepted: December 30, 2021
Published: February 18, 2022

REFERENCES

Baldwin, P., Likhotvorik, R., Baig, N., Cropper, J., Carlson, R., Kurmasheva, R., and Sridhar, S. (2019). Nanoformulation of talazoparib increases maximum tolerated doses in combination with temozolomide for treatment of ewing sarcoma. Front Oncol. *9*, 1416.

Beckford Vera, D.R., Fontaine, S.D., Vanbrocklin, H.F., Hearn, B.R., Reid, R., Ashley, G.W., and Santi, D.V. (2020). PET imaging of the EPR effect in tumor xenografts using small 15 nm diameter polyethylene glycols labeled with zirconium-89. Mol. Cancer Ther. *19*, 673–679.

Bliss, C. (1939). The toxicity of poisons applied jointly. Ann. Appl. Biol. *26*, 585–615.

Britten, C.D., Rowinsky, E.K., Baker, S.D., Agarwala, S.S., Eckardt, J.R., Barrington, R., Diab, S.G., Hammond, L.A., Johnson, T., Villalona-Calero, M., et al. (1999). A Phase I and pharmacokinetic study of temozolomide and cisplatin in patients with advanced solid malignancies. Clin. Cancer Res. *5*, 1629–1637.

Caster, J.M., Sethi, M., Kowalczyk, S., Wang, E., Tian, X., Nabeel Hyder, S., Wagner, K.T., Zhang, Y.A., Kapadia, C., Man Au, K., and Wang, A.Z. (2015). Nanoparticle delivery of chemosensitizers improve chemotherapy efficacy without incurring additional toxicity. Nanoscale *7*, 2805–2811.

Chauhan, V.P., and Jain, R.K. (2013). Strategies for advancing cancer nanomedicine. Nat. Mater. *12*, 958–962.

Chauhan, V.P., Stylianopoulos, T., Martin, J.D., Popovic, Z., Chen, O., Kamoun, W.S., Bawendi, M.G., Fukumura, D., and Jain, R.K. (2012). Normalization of tumour blood vessels improves the delivery of nanomedicines in a size-dependent manner. Nat. Nanotechnol *7*, 383–388.

Donaldson, S.S., Torrey, M., Link, M.P., Glicksman, A., Gilula, L., Laurie, F., Manning, J., Neff, J., Reinus, W., Thompson, E., and Shuster, J.J. (1998). A multidisciplinary study investigating radiotherapy in Ewing's sarcoma: end results of POG #8346. Pediatric Oncology Group. Int. J. Radiat. Oncol. Biol. Phys. *42*, 125–135.

Drew, Y., Ledermann, J., Hall, G., Rea, D., Glasspool, R., Highley, M., Jayson, G., Sludden, J., Murray, J., Jamieson, D., et al. (2016). Phase 2 multicentre trial investigating intermittent and continuous dosing schedules of the poly(ADP-ribose) polymerase inhibitor rucaparib in germline BRCA mutation carriers with advanced ovarian and breast cancer. Br. J. Cancer *114*, 723–730.

Dunst, J., Jurgens, H., Sauer, R., Pape, H., Paulussen, M., Winkelmann, W., and Rube, C. (1995). Radiation therapy in Ewing's sarcoma: an update of the CESS 86 trial. Int. J. Radiat. Oncol. Biol. Phys. *32*, 919–930.

Ferrari, S., Mercuri, M., Rosito, P., Mancini, A., Barbieri, E., Longhi, A., Rimondini, S., Cesari, M., Ruggieri, P., Di Liddo, M., and Bacci, G. (1998). Ifosfamide and actinomycin-D, added in the induction phase to vincristine, cyclophosphamide and doxorubicin, improve histologic response and prognosis in patients with non metastatic Ewing's sarcoma of the extremity. J. Chemother. *10*, 484–491.

Fontaine, S.D., Ashley, G.W., Houghton, P.J., Kurmasheva, R.T., Diolaiti, M., Ashworth, A., Peer, C.J., Nguyen, R., Figg, W.D., et al. (2021). A very long-acting PARP inhibitor suppresses cancer cell growth in DNA repair-deficient tumor models. Cancer Res. *81*, 1076–1086.

Fontaine, S.D., Hann, B., Reid, R., Ashley, G.W., and Santi, D.V. (2019). Species-specific optimization of PEG∼SN-38 prodrug pharmacokinetics and antitumor effects in a triple-negative BRCA1-deficient xenograft. Cancer Chemother. Pharmacol. *84*, 729–738.

Ghilu, S., Li, Q., Fontaine, S.D., Santi, D.V., Kurmasheva, R.T., Zheng, S., and Houghton, P.J. (2020). Prospective use of the single-mouse experimental design for the evaluation of PLX038A. Cancer Chemother. Pharmacol. *85*, 251–263.

Grier, H.E., Krailo, M.D., Tarbell, N.J., Link, M.P., Fryer, C.J., Pritchard, D.J., Gebhardt, M.C., Dickman, P.S., Perlman, E.J., Meyers, P.A., et al. (2003). Addition of ifosfamide and etoposide to standard chemotherapy for Ewing's sarcoma and primitive neuroectodermal tumor of bone. N. Engl. J. Med. *348*, 694–701.

Houghton, K.R., Erickson, S., Smith, M., Lock, R., Evans, K., and Toscan, C. (2020). Prospective Validation of Single Mouse Testing (SMT) by the Pediatric Preclinical Testing Consortium (PPTC). EORTC/AACR/NCI Molecular Targets Meeting (virtual). https://doi.org/10.1016/S0959-8049(20)31111-4.

Houghton, P.J., Morton, C.L., Tucker, C., Payne, D., Favours, E., Cole, C., Gorlick, R., Kolb, E.A., Zhang, W., Lock, R., et al. (2007). The pediatric preclinical testing program: description of models and early testing results. Pediatr. Blood Cancer *49*, 928–940.

Kendsersky, N.M., Lindsay, J., Kolb, E.A., Smith, M.A., Teicher, B.A., Erickson, S.W., Earley, E.J., Mosse, Y.P., Martinez, D., Pogoriler, J., et al. (2021). The B7-H3-targeting antibody-drug conjugate m276-SL-PBD is potently effective against pediatric cancer preclinical solid tumor models. Clin. Cancer Res. *27*, 2938–2946.

Kolb, E.A., Kushner, B.H., Gorlick, R., Laverdiere, C., Healey, J.H., Laquaglia, M.P., Huvos, A.G., Qin, J., Vu, H.T., Wexler, L., et al. (2003). Long-term event-free survival after intensive chemotherapy for Ewing's family of tumors in children and young adults. J. Clin. Oncol. *21*, 3423–3430.

Krasin, M.J., Rodriguez-Galindo, C., Billups, C.A., Davidoff, A.M., Neel, M.D., Merchant, T.E., and Kun, L.E. (2004). Definitive irradiation in multidisciplinary management of localized Ewing sarcoma family of tumors in pediatric patients: outcome and prognostic factors. Int. J. Radiat. Oncol. Biol. Phys. *60*, 830–838.

Maeda, H., Wu, J., Sawa, T., Matsumura, Y., and Hori, K. (2000). Tumor vascular permeability and the EPR effect in macromolecular therapeutics: a review. J. Control Release *65*, 271–284.

Matsumura, Y., and Maeda, H. (1986). A new concept for macromolecular therapeutics in cancer chemotherapy: mechanism of tumoritropic accumulation of proteins and the antitumor agent smancs. Cancer Res. *46*, 6387–6392.

Middlemas, D.S., Stewart, C.F., Kirstein, M.N., Poquette, C., Friedman, H.S., Houghton, P.J., and Brent, T.P. (2000). Biochemical correlates of temozolomide sensitivity in pediatric solid tumor xenograft models. Clin. Cancer Res. *6*, 998–1007.

Murphy, B., Yin, H., Maris, J.M., Kolb, E.A., Gorlick, R., Reynolds, C.P., Kang, M.H., Keir, S.T., Kurmasheva, R.T., Dvorchik, I., et al. (2016). Evaluation of alternative in vivo drug screening methodology: a single mouse analysis. Cancer Res. *76*, 5798–5809.

Neale, G., Su, X., Morton, C.L., Phelps, D., Gorlick, R., Lock, R.B., Reynolds, C.P., Maris, J.M., Friedman, H.S., Dome, J., et al. (2008). Molecular characterization of the pediatric preclinical testing panel. Clin. Cancer Res. *14*, 4572–4583.

Portnow, J., Badie, B., Chen, M., Liu, A., Blanchard, S., and Synold, T.W. (2009). The neuropharmacokinetics of temozolomide in patients with resectable brain tumors: potential implications for the current approach to chemoradiation. Clin. Cancer Res. *15*, 7092–7098.

Potratz, J., Dirksen, U., Jurgens, H., and Craft, A. (2012). Ewing sarcoma: clinical state-of-the-art. Pediatr. Hematol. Oncol. *29*, 1–11.

Rokita, J.L., Rathi, K.S., Cardenas, M.F., Upton, K.A., Jayaseelan, J., Cross, K.L., Pfeil, J., Egolf, L.E., Way, G.P., Farrel, A., et al. (2019). Genomic profiling of childhood tumor patient-derived xenograft models to enable rational clinical trial design. Cell Rep *29*, 1675–1689.e9.

Schafer, E.S., Rau, R.E., Berg, S.L., Liu, X., Minard, C.G., Bishop, A.J.R., Romero, J.C., Hicks, M.J., Nelson, M.D., Jr., Voss, S., et al. (2020). Phase 1/2 trial of talazoparib in combination with temozolomide in children and adolescents with refractory/recurrent solid tumors including Ewing sarcoma: a Children's Oncology Group Phase 1 Consortium study (ADVL1411). Pediatr. Blood Cancer *67*, e28073.

Shen, Y., Rehman, F.L., Feng, Y., Boshuizen, J., Bajrami, I., Elliott, R., Wang, B., Lord, C.J., Post, L.E., and Ashworth, A. (2013). BMN 673, a novel and highly potent PARP1/2 inhibitor for the treatment of human cancers with DNA repair deficiency. Clin. Cancer Res. *19*, 5003–5015.

Smith, M.A., Reynolds, C.P., Kang, M.H., Kolb, E.A., Gorlick, R., Carol, H., Lock, R.B., Keir, S.T., Maris, J.M., Billups, C.A., et al. (2015). Synergistic activity of PARP inhibition by talazoparib (BMN 673) with temozolomide in pediatric cancer models in the pediatric preclinical testing program. Clin. Cancer Res. *21*, 819–832.

Tsouris, V., Joo, M.K., Kim, S.H., Kwon, I.C., and Won, Y.Y. (2014). Nano carriers that enable co-delivery of chemotherapy and RNAi agents for treatment of drug-resistant cancers. Biotechnol. Adv. *32*, 1037–1050.

Van De Ven, A.L., Tangutoori, S., Baldwin, P., Qiao, J., Gharagouzloo, C., Seitzer, N., Clohessy, J.G., Makrigiorgos, G.M., Cormack, R., Pandolfi, P.P., and Sridhar, S. (2017). Nanoformulation of Olaparib amplifies PARP inhibition and sensitizes PTEN/TP53-deficient prostate cancer to radiation. Mol. Cancer Ther. *16*, 1279–1289.

Yang, S., Wallach, M., Krishna, A., Kurmasheva, R., and Sridhar, S. (2021). Recent developments in nanomedicine for pediatric cancer. J. Clin. Med. *10*, 1437.

STAR★METHODS

KEY RESOURCES TABLE

REAGENT or RESOURCE	SOURCE	IDENTIFIER
Antibodies		
PARP1 (46D11) Rabbit mAb	Cell Signaling Technology	Cat#9532; RRID: AB_659884
GAPDH (14C10) Rabbit mAb	Cell Signaling Technology	Cat#2118; RRID: AB_561053
IRDye 680RD Goat anti-Mouse IgG Secondary Antibody	LI-COR Biotechnology	Cat#926-68070; RRID: AB_10956588; Lot#C70613-15
IRDye 800CW Goat anti-Rabbit IgG Secondary Antibody	LI-COR Biotechnology	Cat#926-32211; RRID: AB_621843; Lot#C70620-05
Biological samples		
EW-5 patient-derived xenograft	Ghilu et al., 2020	N/A
EW-10 patient-derived xenograft	Houghton et al., 2007	N/A
EW-13 patient-derived xenograft	Houghton et al., 2007	N/A
NCH-EWS1 patient-derived xenograft	Ghilu et al., 2020	N/A
ES-1 cell line-derived xenograft	Houghton et al., 2007	N/A
ES-2 cell line-derived xenograft	Houghton et al., 2007	N/A
ES-3 cell line-derived xenograft	Houghton et al., 2007	N/A
ES-4 cell line-derived xenograft	Houghton et al., 2007	N/A
ES-6 cell line-derived xenograft	Houghton et al., 2007	N/A
ES-7 cell line-derived xenograft	Houghton et al., 2007	N/A
TC-71 cell line-derived xenograft	Houghton et al., 2007	N/A
CHLA-258 cell line-derived xenograft	Houghton et al., 2007	N/A
SK-NEP-1 cell line-derived xenograft	Houghton et al., 2007	N/A
EW-8 cell line-derived xenograft	Houghton et al., 2007	N/A
Rh-28 patient-derived xenograft	Ghilu et al., 2020	N/A
Rh-30R patient-derived xenograft	Ghilu et al., 2020	N/A
Rh-41 patient-derived xenograft	Ghilu et al., 2020	N/A
Rh-65 patient-derived xenograft	Ghilu et al., 2020	N/A
Rh-73 patient-derived xenograft	Houghton et al., 2007	N/A
Rh-80 patient-derived xenograft	Houghton et al., 2007	N/A
Rh-82 patient-derived xenograft	Houghton et al., 2007	N/A
Rh-88 patient-derived xenograft	Houghton et al., 2007	N/A
KT-16 patient-derived xenograft	Houghton et al., 2007	N/A
NCH-RBD2 patient-derived xenograft	Houghton et al., 2007	N/A
KT-14 patient-derived xenograft	Houghton et al., 2007	N/A
Rh-18 patient-derived xenograft	Ghilu et al., 2020	N/A
OS-46 patient-derived xenograft	Houghton et al., 2007	N/A
Aska-SS cell line-derived xenograft	Cells purchased from Riken Cell Bank	RCB3576
Yamato-SS cell line-derived xenograft	Cells purchased from Riken Cell Bank	RCB3577
HS-SY-II cell line-derived xenograft	Cells purchased from Riken Cell Bank	RCB2231
GBM2 patient-derived xenograft	Houghton et al., 2007	N/A
Chemicals, peptides, and recombinant proteins		
PEG~TLZ	Prolynx, LLC	PLX376 (prolynxinc.com)
PEG_{40kDa}-$[NH_2]_4$	NOF America	Sunbright PTE-400PA; CAS: 804514-67-8
Temozolomide	MedChemExpress	HY-17364; CAS: 85622-93-1

(*Continued on next page*)

Continued

REAGENT or RESOURCE	SOURCE	IDENTIFIER
Critical commercial assays		
Alamar Blue	Bio-Rad Laboratories	Cat#BUF012B
Experimental models: Cell lines		
A-673 human cell line	Cells purchased from ATCC	Cat#CRL-1598; RRID: CVCL_0080
ES-2 human cell line	Houghton et al., 2007	RRID:CVCL_AX39
ES-4 human cell line	Houghton et al., 2007	RRID:CVCL_1200
ES-6 human cell line	Houghton et al., 2007	RRID:CVCL_1202
ES-7 human cell line	Houghton et al., 2007	RRID:CVCL_1203
EW-8 human cell line	Houghton et al., 2007	RRID:CVCL_V618
TC-71 human cell line	Houghton et al., 2007	RRID:CVCL_S882
CHLA-258 human cell line	Houghton et al., 2007	RRID:CVCL_A058
Experimental models: Organisms/strains		
Mouse: C.B-*Igh-1*^{b}/IcrTac-*Prkdc*^{scid}	Envigo (Indianapolis IN)	Item # 18205F

RESOURCE AVAILABILITY

Lead contact

Further information and requests for resources and reagents should be directed to and will be fulfilled by the lead contact, Raushan Kurmasheva (Kurmasheva@uthscsa.edu).

Materials availability statement

This study did not generate new unique reagents.

Data and code availability

- All data reported in this paper will be shared by the lead contact upon request.
- This paper does not report original code.
- Any additional information required to reanalyze the data reported in this paper is available from the lead contact upon request.

EXPERIMENTAL MODEL AND SUBJECT DETAILS

Ewing sarcoma cell lines and solid tumor xenograft models

Ewing sarcoma cell lines (TC-71, EW-8, ES-2, ES-4, ES-6, ES-7, A673, and CHLA-258) were cultured in RPMI-1640 medium (*SH30027.02, HyClone*) supplemented with 10% heat-inactivated fetal bovine serum (FBS, *F-4135, Millipore Sigma*). These Ewing sarcoma cell lines were derived from xenograft tumors, and are male (TC-71, EW-8, ES-4, ES-6, ES-7) or female (ES-2, CHLA-258) origin. The A673 cell line was purchased from the American Type Culture Collection (*Manassas, VA*) and are of female origin. Cells were maintained at 37°C in a humidified atmosphere with 5% CO_2. All cell lines were authenticated by short tandem repeat (STR) analysis using the PowerPlex® 16 System (a multiplex STR system for use in DNA typing) for sample analysis on the Applied Biosystems Genetic Analyzer 3730 and were free of mycoplasma contamination. The *EWSR1-FLI1* fusion type for each cell line is shown in Table S1. Generally, a cell line reaching a passage number over 30 is discontinued and an earlier cryopreserved passage cell line is used instead. Patient- and cell line-derived (PDX and CDX) Ewing sarcoma, glioblastoma, Wilms tumor, malignant rhabdoid tumor, rhabdomyosarcoma, osteosarcoma, and synovial sarcoma xenograft models were developed in PPTP [Houghton et al., 2007] or from cell lines (synovial sarcoma). *In vivo* testing was performed using C.B-*Igh-1*^{b}/IcrTac-*Prkdc*^{scid} female mice (*Envigo*, Indianapolis, IN) of 6-8 weeks old. The demographic data for models used in the studies are presented in Table S2. All evaluated tumor models were authenticated by short tandem repeat (STR) analysis against reference profiles and have been described previously (Houghton et al., 2007).

METHOD DETAILS

In vitro cytotoxicity assay

The cytotoxic potencies of PEG∼TLZ (*Prolynx, Inc.*), TMZ (*MedChemExpress, HY-17364*), and PEG∼TLZ + TMZ against Ewing sarcoma cell lines were evaluated by Alamar Blue assays (*BUF012, Bio-Rad laboratories*). Cells were plated in 96-well plates at 3.33×10^3 cells/well, allowed to adhere overnight, and treated with vehicle (0.5% DMSO for TMZ and isotonic acetate buffer (pH 5) for PEG∼TLZ) or drug for 72 h. Alamar Blue (10% of culture volume) was added to each well for 6 h and fluorescence was measured at 590 nm (excitation 570 nm) on a PHERAstar microplate reader (*BMG Labtech*). All samples were blank-corrected for the background fluorescence of Alamar Blue. Concentration-response curves were plotted and IC_{50} values were interpolated from nonlinear regressions using Prism 9 (*GraphPad software*). Combination indexes (CI) were calculated on the basis of the Bliss model of independence using the formula: $CI = (E_A + E_B - E_AE_B)/E_{AB}$, where ($E_A$, E_B) equal the effects of each individual drug and (E_{AB}) equals the effect of the drugs in combination.

Protein extraction and immunoblotting

Cells were treated for 24 h and 48 h with vehicle, TLZ (IC_{50}), TMZ (IC_{50}) or PEG∼TLZ + TMZ (IC_{50} of each) and total protein was extracted with cell lysis buffer (*Cell Signaling Technology, #9803*) containing Halt Protease Inhibitor Cocktail (*Thermo Fisher Scientific*) and 1 mmol/L phenylmethylsulfonylfluoride (*Sigma-Aldrich*). Protein concentrations of each lysate were measured with a Protein Assay Kit (*Bio-Rad Laboratories*) and 10 μg of total protein was separated on NuPAGE 4% to 12% Bis-Tris gels (*Thermo Fisher Scientific*). Proteins were transferred to Immobilon-FL PVDF membranes (*MilliporeSigma*) and probed with antibodies for PARP1 (*Cell Signaling Technology #9532*) and GAPDH (*Cell Signaling Technology #2118*). Primary antibodies were diluted in Odyssey Blocking Buffer (LI-COR) with 0.1% Tween 20 (*Sigma-Aldrich*). Membranes were incubated with IRDye 680 or IRDye 800CW-conjugated secondary antibodies (LI-COR) diluted in Odyssey Blocking Buffer with 0.1% Tween 20 and 0.01% SDS. Fluorescence was detected with an Odyssey CLx Imaging System and analyzed with Image Studio software (LI-COR).

Drugs and formulation

PEG∼TLZ was provided by ProLynx Inc. (San Francisco) and prepared according to approaches described earlier, and TLZ was purchased from ApexBio and MedKoo (*A4153; 204,710*) (Fontaine et al., 2019, 2021). Drug formulations were made in isotonic acetate buffer (pH 5) and sterile filtered through a 0.2 μm filter. Formulated PEG∼TLZ was stored at −80°C and thawed immediately prior to use. PEG∼TLZ was administered as a single intraperitoneal (I.P.) administration at 5, 10, and 20 μmol/kg. TMZ was administered per orally (P.O.) at 30 and 40 mg/kg on day 3 or 4 following PEG∼TLZ, for five consecutive days.

In vivo testing

Mice were maintained under barrier conditions and experiments were conducted using protocols and conditions approved by The Institutional Animal Care and Use Committee (# 15015) at UT Health San Antonio. *In vivo* methods developed in the PPTP (Houghton et al., 2007) were used in this study. All animal handling procedures (tumor transplantation, drug formulation and administration, tumor measurement, etc.) were undertaken in the class 2 biological safety cabinet. Immunocompromised mice were housed in sterile cages with sterile bedding (5 mice/cage) and provided irradiated commercial pelleted diet and sterile, acidified water in bottles *ad libitum*. The room temperature was maintained at 21-26°C, relative humidity between 30 and 70%, and with a 14:10 day: night light cycle. Mice were selected for efficacy studies when tumors were 200–400 mm^3. Regrowth of tumors was determined following tumor regression. Endpoints were time to event (defined as tumor growing to 400% of its volume at the initiation of treatment), EFS, and percent tumor regression. Complete Regression (CR) was defined as tumor volume <40 mm^3.

QUANTIFICATION AND STATISTICAL ANALYSIS

In vitro studies

The expected effects of each combination of PEG∼TLZ and TMZ were calculated by adding the individual effects of each drug. The expected effects were compared to the actual effect of the combination using multiple unpaired t-tests with Holm-Šídák corrections for multiple comparisons. All statistical testing was 2-sided and was performed with an experimentwise significance level of 5% using Prism 9. All error bars in Figure 1 represent mean ± standard error of the mean for n = 3 independent experiments, with each concentration tested in triplicate.

In vivo studies

All error bars in graphs for Figures 3 and 4 represent standard error of the mean for groups of 5 or 10 mice. Paired control and treated EFS distributions were described with Kaplan Meier curves (Figure 5B). The detailed description of the *in vivo* statistical analytic methods used in Figures 3, 4, and 5 is presented here: An *event* is defined as a quadrupling of tumor volume from day 0. The exact time-to-event is estimated by interpolating between the measurements directly preceding and following the event, assuming log-linear growth. The significance of differences in EFS between experimental groups (e.g., treated vs controls) was assessed with log rank tests. The significance of variation in EFS with group (control vs treated) in SMT data was assessed with a proportional hazards model for paired survival data; EFS distributions were summarized graphically with Kaplan-Meier curves. All statistical testing was 2-sided with a significance level of 5%. Corrections for multiple comparisons were not applied. The software packages R and SAS were used throughout.

The *objective response* categories are progressive disease (PD, which is subdivided into progressive disease without and with growth delay, PD1 and PD2 respectively, defined only for treated mice), stable disease (SD), partial response (PR), complete response (CR), and maintained complete response (MCR). For solid tumor experiments, objective response categories are defined as follows: PD when <50% tumor regression throughout study and >25% tumor growth at end of study; PD1 when PD and the mouse's time to event $\leq$200% the KM median time-to-event in control group; PD2 when PD but, additionally, time-to-event is >200% of the Kaplan-Meier (KM) median time-to-event in control group; SD when <50% tumor regression throughout study and $\leq$25% tumor growth at end of study; PR when $\geq$50% tumor regression at any point during study, but measurable tumor throughout study period; CR when disappearance of measurable tumor mass during the study period; MCR when no measurable tumor mass for at least 3 consecutive weekly readings at any time after treatment has been completed.

Overall group response is determined by the median response among evaluable mice as follows: Each individual mouse is assigned a score from 0 to 10 based on its response: PD1 = 0, PD2 = 2, SD = 4, PR = 6, CR = 8, and MCR = 10, and the median for the group determines the overall response. If the median score is half-way between two objective response number categories, the objective response is assigned to the lower response category (e.g., an objective response score of 9 is scored CR). Studies in which toxicity is >25%, or in which the control group is not SD or worse, are considered unevaluable and are excluded from analysis. Treatment groups with PR, CR, or MCR are considered to have had an objective response. Agents inducing objective responses are considered highly active against the tested line, while agents inducing SD or PD2 are considered to have intermediate activity, and agents producing PD1 are considered to have a low level of activity against the tested line. For the single mouse testing (SMT), we report time-to-event, area over the curve (AOC), minimum relative tumor volume (RTV), and the objective response measure for each PDX or CDX model tested. For combination testing, the primary objective is generally to demonstrate that the combination is significantly more effective than either agent utilized at its optimal single agent dose/schedule. This condition is termed therapeutic enhancement, which represents a therapeutic effect for which a tolerated regimen of a combination treatment exceeds the optimal effect achieved at any tolerated dose of monotherapy associated with the same drugs used in the combination. This definition is operationalized as follows: therapeutic enhancement is considered present when the tumor growth delay (T-C) for a combination is greater than the tumor growth delay for each of the single agents tested at their maximum tolerated dose (MTD) and when the EFS distribution for the combination treatment is significantly better than the EFS distributions for both of the single agents tested at their MTD. In order to control experiment-wise Type I error at 5%, statistical tests are evaluated at the Bonferroni-corrected significance level $\alpha = 0.01$ due to the five comparisons being made (combination vs. agent 1 alone, combination vs. agent 2 alone, agent 1 vs. control, agent 2 vs. control, and combination vs. control). Testing is considered not evaluable for therapeutic enhancement if either single agent used alone produces a median EFS beyond the observation period. If a treatment group exhibits excessive toxicity (>25% toxic deaths), therapeutic enhancement is not evaluated.